PROCEEDINGS, 51st Workshop on Geothermal Reservoir Engineering
Stanford University, Stanford, California, February 9-11, 2026
SGP-TR-230

# Techno-Economic Viability of Next Generation Geothermal Resources Across the Temperature Spectrum: A Comparative Analysis with Superhot Rock

Jonathan Pezzino

Scientific Web Services LLC, Seattle, Washington

jonathan@scientificwebservices.com

**Keywords:** EGS, SHR, techno-economic analysis, LCOE, IRR, GEOPHIRES

## ABSTRACT

Levelized Cost of Electricity (LCOE), Internal Rate of Return (IRR), and other techno-economic metrics were computed for a 500 MWe Enhanced Geothermal System (EGS) project in 294 scenarios across temperatures ranging from 200–450°C, gradients from 28.3–112°C/km, and 2 drilling and completion cost models representing FOAK (First-of-a-Kind) and NOAK (Nth-of-a-Kind) approaches.

Results indicate that Superhot Rock (SHR) EGS may yield approximately 43% lower LCOE and 246% higher IRR compared to 200°C in NOAK scenarios. The gradient-weighted average SHR IRR of 34.5% is 24.5 percentage points greater than the gradient-weighted average Baseline IRR of 9.98%, a 246% relative increase. This is primarily driven by the higher enthalpy of SHR fluids, which increases net power production per well up to 520% and thereby reduces the total number of wells required by up to 84%.

Furthermore, the analysis indicates that for high geothermal gradients, SHR may yield compelling returns even in present-day FOAK scenarios, with the IRR increasing by 21 percentage points or more compared to lower-temperature EGS.

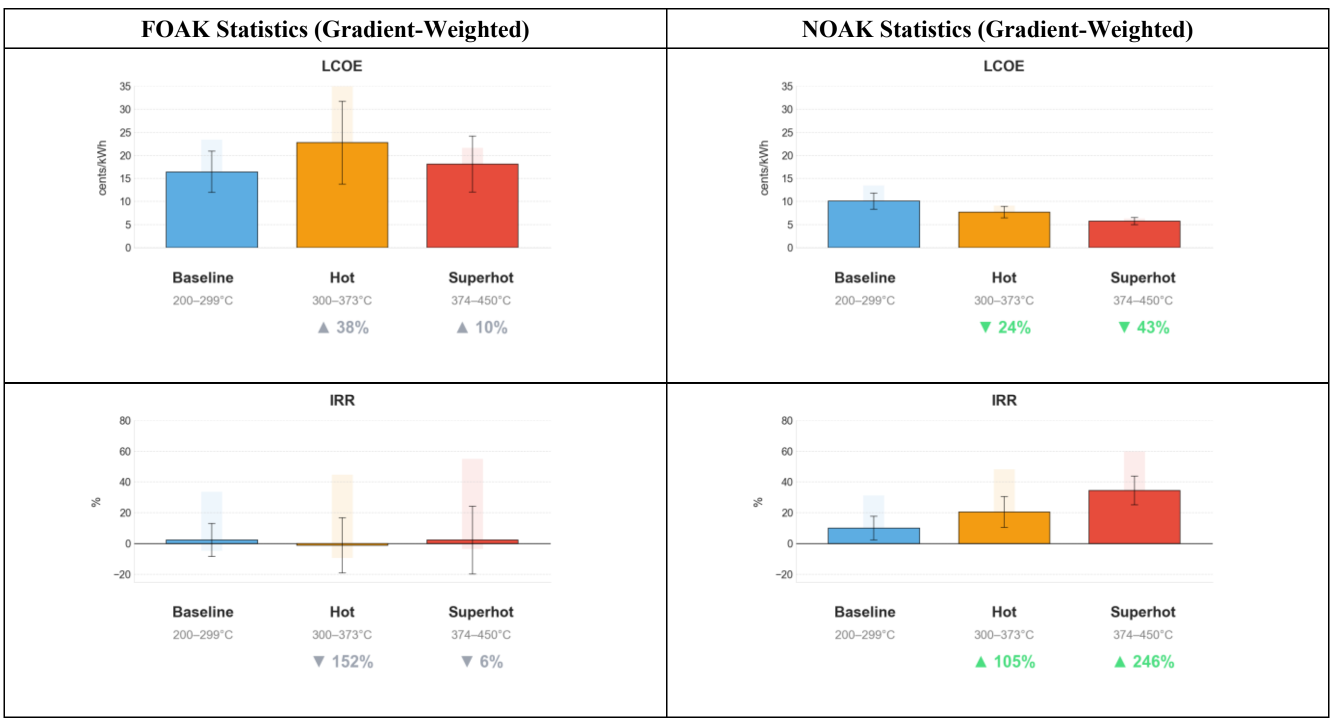

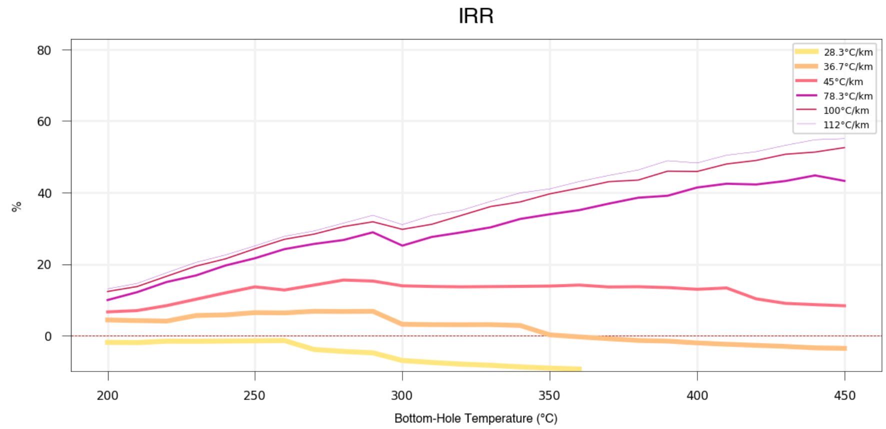


**Figure 0: First-of-a-Kind (FOAK) scenario internal rate of return (IRR) results by bottom-hole temperature and gradient, demonstrating compelling present-day SHR EGS returns for high geothermal gradients.**

## 1. INTRODUCTION

Rapidly growing electricity demand, driven by widespread electrification and the expansion of energy-intensive computing for applications like artificial intelligence, has created a critical need for scalable, zero-carbon, firm power sources. Geothermal energy, with its high capacity factor and low land-use footprint, is a promising candidate to meet this need. Conventional hydrothermal resources, however, are geographically limited. Enhanced Geothermal Systems (EGS) aim to overcome this limitation by engineering reservoirs in hot rock, vastly expanding the potential resource base.

Within the EGS landscape, Superhot Rock (SHR) systems, targeting temperatures above 374°C, represent a significant technological frontier. The higher enthalpy of fluids produced from SHR reservoirs offers the potential for substantially greater power output per well, which could lead to dramatically improved project economics. However, accessing these high-temperature resources also presents considerable technical and financial challenges, particularly related to deep drilling and reservoir stimulation in extreme temperature, pressure and geochemical conditions. Consequently, the economic viability of SHR EGS, especially in the near term, remains a critical uncertainty for developers, investors, and policymakers.

To address this knowledge gap, this paper presents a detailed techno-economic analysis of a utility-scale (500 MWe) SHR EGS project. Using the GEOPHIRES techno-economic simulator, we model project performance and financial metrics, including Levelized Cost of Electricity (LCOE) and Internal Rate of Return (IRR), across a wide range of geological conditions and cost assumptions. The analysis explicitly compares SHR economics to lower-temperature EGS across two distinct development timelines: a near-term, First-of-a-Kind (FOAK) model and a mature, Nth-of-a-Kind (NOAK) model.

## 2. METHODOLOGY

Techno-economic results including LCOE and IRR were calculated using GEOPHIRES for a 500 MWe EGS project in 26 bottom-hole temperature tranches ranging from 200°C to 450°C in 10°C increments, 6 gradient tranches from 28.3°C/km to 112°C/km, and 2 drilling and completion cost model tranches representing FOAK and NOAK. (294 total scenarios).

### GEOPHIRES Simulator

GEOPHIRES (github.com/NREL/GEOPHIRES-X) is a free and open-source geothermal techno-economic simulator maintained by the National Renewable Energy Laboratory (NREL) and other contributors including Scientific Web Services LLC (SWS). Various reservoir conditions and end-use options can be modeled, including low- and high-temperature enhanced geothermal systems (SHR EGS) (Beckers & McCabe, 2019). GEOPHIRES v3.9 was used to perform techno-economic analysis for this study (NREL, 2025).

### EGS Project Base Case

An EGS project base case was defined for parameters that were kept constant across tranches. The base case was adapted from the "Fervo Cape Station 4" GEOPHIRES example scenario, a case study modeled on extrapolation from available publication data from Fervo Energy and other sources. Base case parameters were formulated for technical compatibility with the analysis tranches (e.g. use of double-flash power plant instead of ORC due to high temperatures), encode analysis assumptions (e.g. 25 year project lifetime), and increase generic applicability of results where possible.

Notable base case parameters and assumptions include the following:

| Parameter | Value | Comment |
|---|---|---|
| Investment Tax Credit Rate | 0% | |

| Parameter | Value | Comment |
|---|---|---|
| Combined Income Tax Rate | 0% | Analysis is performed in a global context without any jurisdiction-specific tax assumptions. |
| Starting Electricity Sale Price | 9.5¢/kWh | Upper end of ranges given in NREL Annual Technology Baseline (ATB) (NREL, 2024) |
| Electricity Escalation Rate Per Year | 0.057¢/kWh | Conservatively calibrated to escalate to 10 cents/kWh at Year 11 (as opposed to calibrating to inflation which would escalate more quickly) |
| Power Plant Type | 4 | Double-Flash |
| Reservoir Model | 1 | Multiple Parallel Fractures Model (Gringarten et al., 1975) |
| Productivity Index | 4.569 kg/s/bar | Equal to ATB Deep EGS Moderate scenario: 2500 lb/hr/psi |
| Injectivity Index | 5.482 kg/s/bar | Equal to ATB Deep EGS Moderate scenario: 3000 lb/hr/psi |
| Maximum Drawdown[1] | 5.31% | Models potential thermal breakthrough requiring redrilling in conjunction with reservoir volume & fracture geometry |
| Water Loss Fraction | 23.75% | Average of 14.5-33% range (Clark et al., 2010) |

Some parameters also differ between FOAK and NOAK base cases, including:

| Parameter | FOAK Value | Comment | NOAK Value | Comment |
|---|---|---|---|---|
| Production Flow Rate per Well | 60 kg/s | NREL ATB conservative and moderate scenarios | 80 kg/s | NREL ATB advanced scenario[2] |
| Discount Rate[3] | 12% | Typical discount rate for high-risk projects might be 12-15% | 7.5% | Lower-risk investment discount rate |

**Scenario Parameters: Temperature and Gradient Tranches**

Bottom-Hole Temperature Tranches

Bottom-hole temperature (BHT) tranches ranged from 200°C to 450°C in 10°C increments.

The precise temperature range of Superhot Rock (SHR) varies across sources but is often defined as a bottom-hole temperature of 374°C or higher. At 374°C, water reaches its supercritical point when pressure is 22 MPa or greater. Hydrostatic reservoir pressure reaches 22 MPa at depths of 2.25 km and higher, meaning initial conditions are expected to be supercritical in most SHR reservoirs. It is not currently known whether pressure will remain at this level over the duration of a typical SHR EGS project, as it may be affected by reservoir engineering and production of fluid from the reservoir. Therefore, reservoir fluid at the bottom of the wellbore may or may not be in the supercritical phase.

This analysis relies on GEOPHIRES v3.9, which calculates fluid properties at the bottom of the wellbore based on the local temperature and pressure. It uses the CoolProp library to determine thermodynamic properties including heat capacity, enthalpy, density, and vapor pressure, which accounts for the fluid's state, whether it is liquid, steam, or supercritical (Bell et al., 2014). However, GEOPHIRES v3.9 does not model potential phase changes or multi-phase flow within the wellbore. Multi-phase production and/or flashing, if they occur, may have positive or negative effects on project economics such as increased flow rate (positive), occurrence of scaling (negative), or higher equipment costs (negative).

Reservoirs containing supercritical fluid are also subject to additional physiochemical factors which were not modeled in this analysis. Supercritical water can be highly corrosive depending on reservoir-specific geochemistry, introducing engineering and equipment challenges that may negatively affect SHR EGS economics (Reinsch et al., 2017). It is also relatively less viscous which may increase flow rates and positively affect economics.

[1] Maximum allowable thermal drawdown before redrilling, expressed as a percentage drop of the initial production temperature (at the wellhead). For example, given an initial production temperature of 200°C and Maximum Drawdown of 5%, redrilling would occur after a 10°C drop in production temperature (to 190°C). See Managing Thermal Drawdown and Redrilling Costs.

[2] This study conservatively uses the ATB's advanced scenario flow rate, but higher flow rates may be possible. NREL's Enhanced Geothermal Shot Analysis models a flow rate of 125 kg/s for flash plants (Augustine et al., 2023).

[3] The Discount Rate serves as a key input for LCOE and net present value (NPV) calculations. IRR, in contrast, is an output metric representing the discount rate at which NPV equals zero.

Note that bottom-hole temperature is always higher than production temperature since heat is lost during transmission to injection fluid (heat extraction), and as production fluid travels up the wellbore. GEOPHIRES's Multiple Parallel Fractures reservoir model (Gringarten et al., 1975) was used to calculate reservoir heat extraction. GEOPHIRES's implementation of Ramey's Wellbore Heat Transmission model (Ramey, 1962) was used to calculate production wellbore temperature drops. For example, a 6.4 km well with BHT of 300°C may yield an average lifetime production temperature of 284.3°C, including an 8.8°C drop predicted by Ramey's model and the remainder owing to heat extraction (Gringarten). The following graph illustrates the relationship between bottom-hole temperature and production temperature for the analysis gradients:

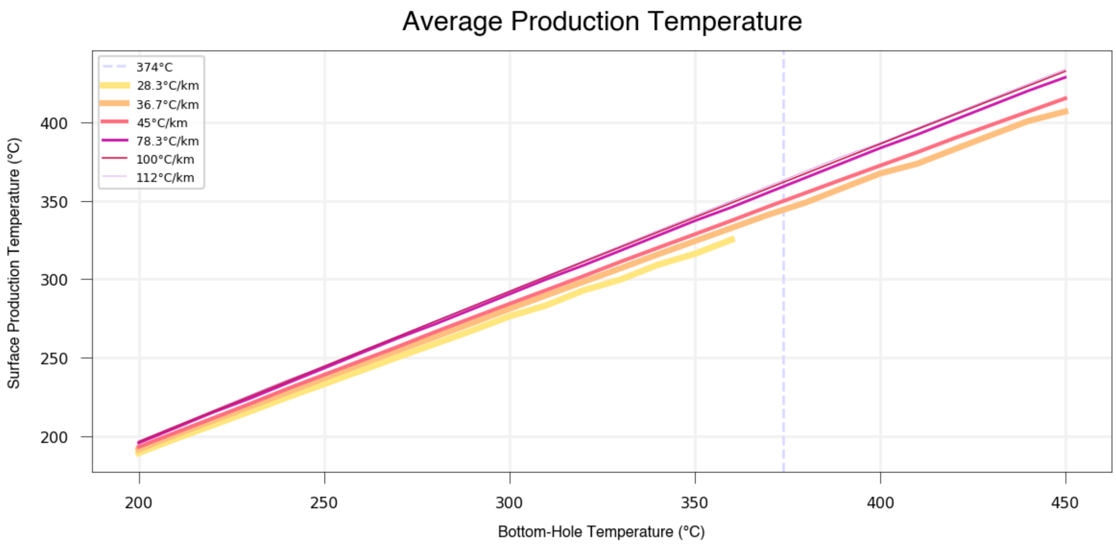


**Figure 1: Average Production Temperature by BHT**

Temperature Buckets

To facilitate a high-level comparison across the temperature spectrum, the results from the individual scenarios were aggregated into the three distinct temperature buckets defined in the table below. These groupings are used in the Statistical Overview sections to present gradient-weighted average results for key metrics like LCOE and IRR. The Baseline bucket serves as the basis against which the Hot and Superhot results are compared.

| Bucket | Bottom-Hole Temperature Range | Legend Color |
|---|---|---|
| Baseline | 200–299°C | (blue) |
| Hot | 300–373°C | (orange) |
| Superhot | 374–450°C | (red) |

Gradient Tranches

Scenarios were generated for gradients from 28.3–112°C/km with the following values:

| Gradient | Legend Color |
|---|---|
| 28.3°C/km | (yellow) |
| 36.7°C/km | (orange) |
| 45.0°C/km | (red) |
| 78.3°C/km | (violet) |
| 100°C/km | (crimson) |
| 112°C/km | (dark violet) |

These values were derived from the bucketing scheme used for the continental US by NREL's Geothermal Prospector (NREL, 2017) using a surface temperature of 12°C, with the addition of 100°C/km and 112°C/km for exceptionally hot sites such as Newberry Volcano and the exclusion of 20°C/km due to its low estimated prevalence and unfavorable EGS economics.

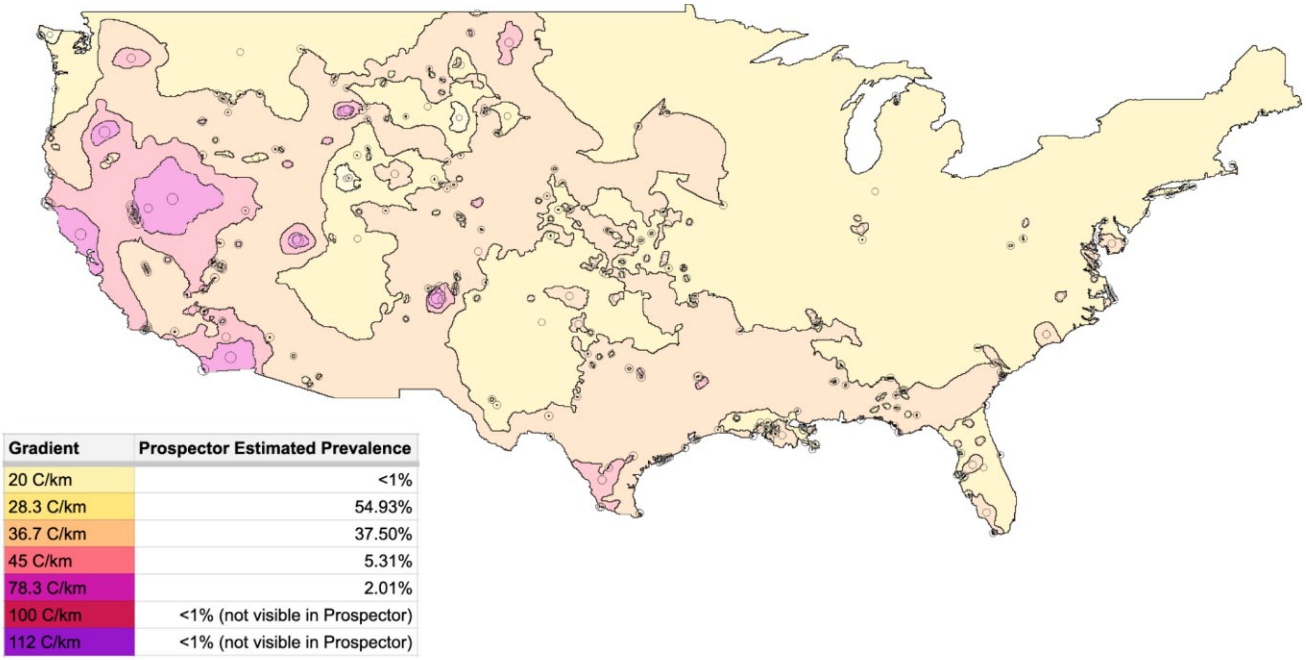

| Gradient | Prospector Estimated Prevalence |
|---|---|
| 20 C/km | <1% |
| 28.3 C/km | 54.93% |
| 36.7 C/km | 37.50% |
| 45 C/km | 5.31% |
| 78.3 C/km | 2.01% |
| 100 C/km | <1% (not visible in Prospector) |
| 112 C/km | <1% (not visible in Prospector) |

**Figure 2: Gradient Prevalence Map: The gradient colors shown correspond to the series colors used in analysis graphs. Series line thickness in analysis graphs corresponds with approximate estimated gradient prevalence in the continental US.**

*Gradient-Weighted Statistics*

To calculate representative values across a large, heterogeneous resource area, this analysis uses statistics weighted according to gradient prevalence, referred to as gradient-weighted statistics in this paper. Because geothermal gradients are not uniformly distributed in reality—lower gradients are often significantly more prevalent than high-quality, hotter gradients—a simple average would be misleading. The gradient-weighted average corrects for this by assigning a weight to the results from each gradient, approximately proportional to its estimated real-world prevalence, as indicated in the Gradient Prevalence Map above. This ensures the final, aggregated metric more realistically reflects the expected outcome for the entire resource.

For example, consider a resource area where a common gradient of 25°C/km accounts for 75% of the land area, while a rarer, high-quality gradient of 50°C/km accounts for the remaining 25%. If the common gradient yields an LCOE of 10¢/kWh and the rare gradient yields an LCOE of 4¢/kWh, the weighted average is calculated as (10¢ × 0.75) + (4¢ × 0.25) = 8.5¢/kWh. This result is significantly different from a simple average of 7¢/kWh, as it correctly reflects the higher prevalence of the less productive gradient in the overall assessment.

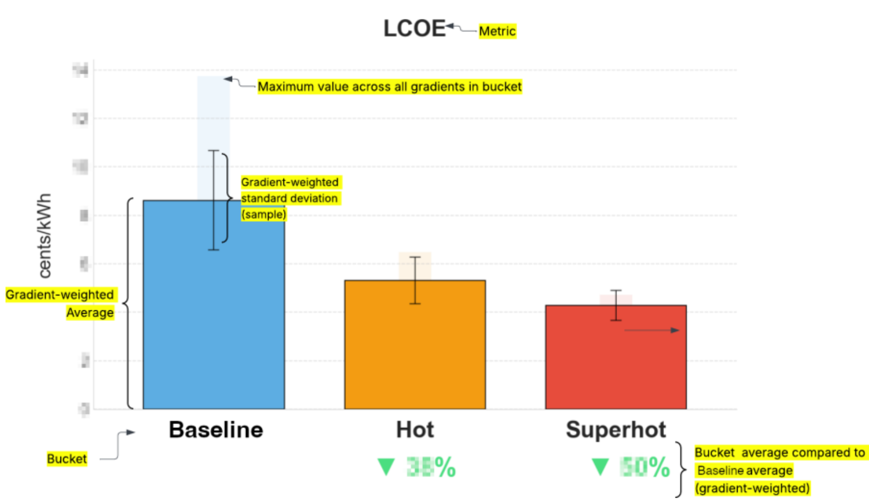


**Figure 3: Gradient-Weighted Statistics Graphs Legend. Thick bars show the gradient-weighted average of all scenarios in the temperature range bucket. Whiskers show the standard deviation. Thin, translucent bars show the minimum and maximum values. The triangular markers and values indicate the average relative to the Baseline average. Note that values shown in this figure are demonstrative only and do not represent analysis results.**

## Subsurface Modeling and Reservoir Design

Reservoir Design

The subsurface system for this analysis is modeled as an array of standardized injector-producer well pairs, or doublets. Each doublet utilizes multi-stage hydraulic fracturing along parallel horizontal laterals to create a large, stimulated rock volume for heat exchange, as visualized in the following figure. A key assumption of this model is that each doublet operates as an independent, hydraulically isolated system, with no thermal or pressure interference from adjacent doublets.

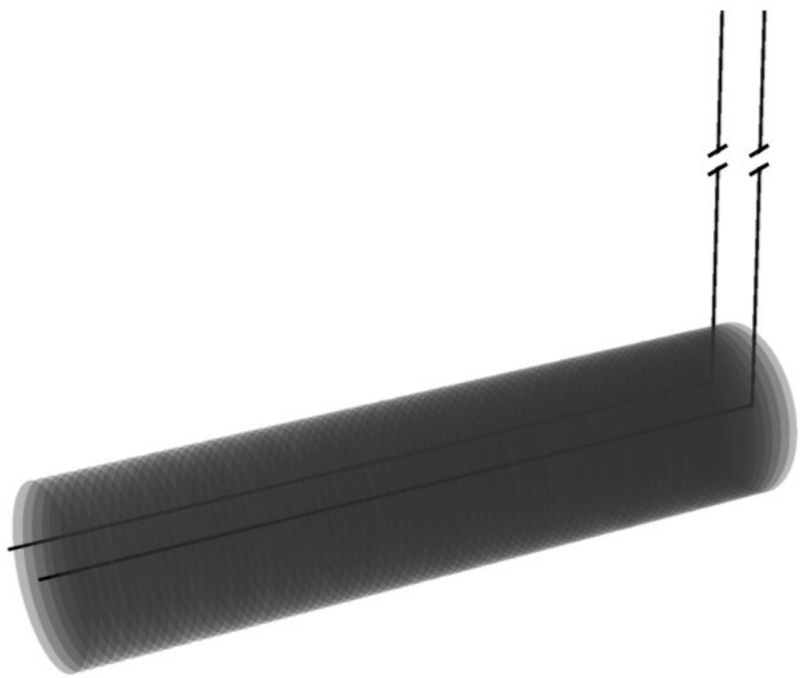

**Figure 4: Visualization of a representative doublet of the analysis reservoir design showing an injection well, production well, and 1440 m laterals with 80 fractures with 18 m spacing. The fractures are shown as 253 m diameter circles for a more physically realistic representation, which have an equivalent surface area to the 224 m square fractures used in the underlying Gringarten reservoir model calculations. Note: for visual clarity, fractures are only shown for the injection well lateral and the vertical wellbores are truncated.**

Drilling Depth

For each temperature-gradient combination, drilling depth to reach the corresponding bottom-hole temperature was calculated. If the drilling depth exceeded 12.5 km (blue dashed line in graph), the scenario was excluded from the analysis. For example, a BHT of 400°C with a gradient of 28.3°C/km would require a depth of 13.7 km, and thus this combination would be excluded.

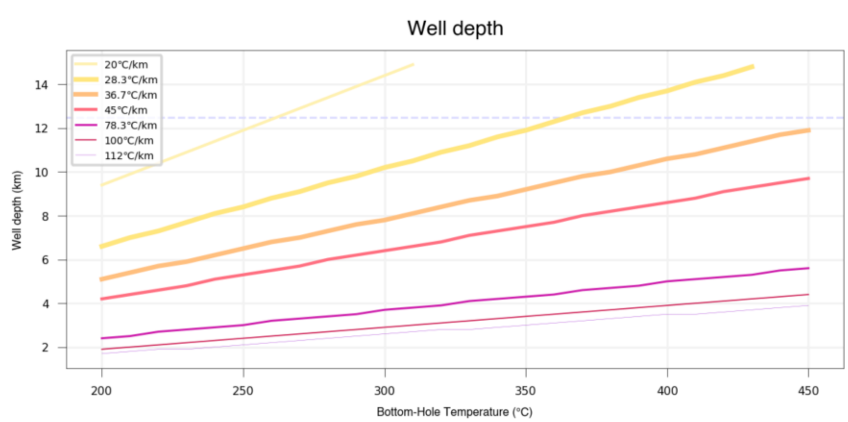


**Figure 5: Required well depth to reach bottom-hole temperature, by gradient.**

500 MWe Power Plant Production Targeting

For each valid temperature-gradient-drilling depth combination, the base case was run in GEOPHIRES with the corresponding parameters, plus parameters for a default number of production/injection well doublets. The number of doublets was then iteratively adjusted until maximum total electricity production of 500 MWe was reached, representing a project analogous to a nominal 2x250 MW turbine plant design. Note that the actual power plant design required for each system may differ from this nominal design due engineering considerations for total flow rate, production temperature, production wellhead pressure, and other factors.

Managing Thermal Drawdown and Redrilling Costs

A critical operational challenge for any enhanced geothermal system is long-term thermal drawdown, where the production temperature, without intervention, declines over the project lifetime. The rate of this decline is primarily a function of the total stimulated reservoir volume and the pace at which heat is extracted relative to the heat flux from the surrounding formation. If unmanaged, this decline can significantly reduce power output over a project's lifetime, jeopardizing its ability to meet contractual obligations, such as a Power Purchase Agreement (PPA). The following figure illustrates how the geofluid temperature and power generation from a single doublet would decay over 25 years.

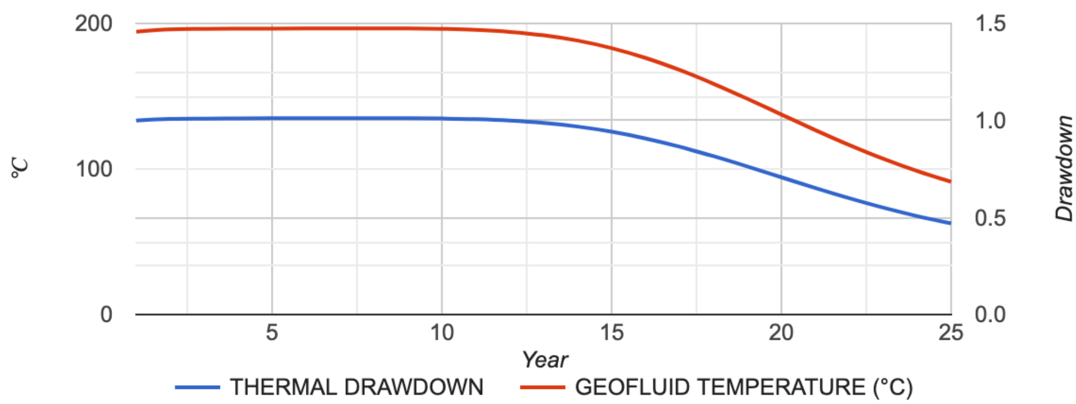


**Figure 6: Simulated 25-year thermal decline for a single EGS well doublet without intervention in the 200°C bottom-hole temperature, 78.3°C/km gradient FOAK scenario. The geofluid temperature (red line, left axis) falls by over 100°C by year 25. The corresponding thermal drawdown (blue line, right axis) represents the production temperature as a fraction of its initial value.**

To counteract this, operators can employ several mitigation strategies, such as managing production flow rates. The strategy leveraged in this analysis is periodic redrilling to access new volumes of hot rock. In GEOPHIRES, this is modeled as discrete events where the entire wellfield is redrilled when production temperature falls by a specified percentage of its initial value, defined by the Maximum Drawdown parameter. Each event simulates accessing a new, undepleted stimulated reservoir volume, which resets the production temperature to its initial value. The cost of a redrilling event is modeled as equivalent to the initial total wellfield cost (including drilling, completion, and stimulation). The cost of all redrilling events is then summed and amortized as an annual operational expense over the project's lifetime.

This analysis models a constant number of redrilling events within each cost model (1 for FOAK, 2 for NOAK), yielding a consistent basis for economic comparison. The result is a stabilized power generation profile for each model, as shown for a representative FOAK scenario in the following figure.

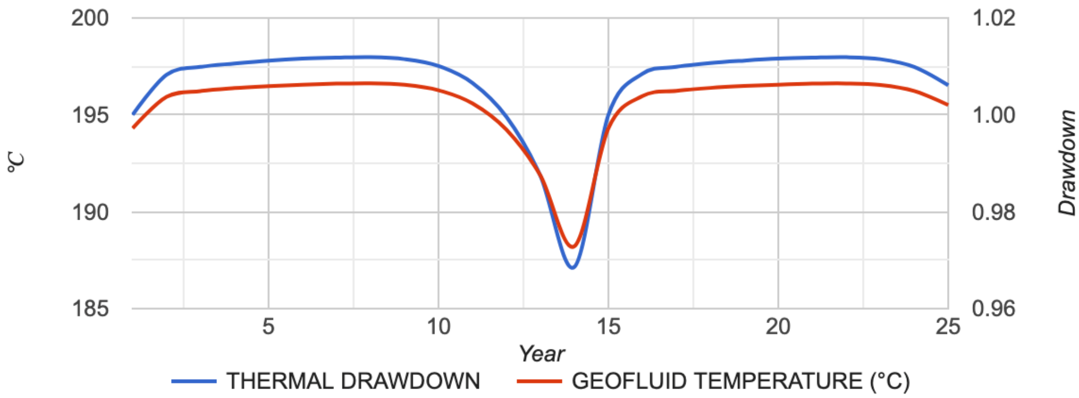


**Figure 7: The modeled power generation profile for a representative FOAK wellfield, showing how a single, planned redrilling event around year 14 successfully mitigates thermal drawdown. The NOAK profile follows a similar pattern but requires two such events to maintain stable output. The geofluid temperature is shown on the left axis, while the thermal drawdown on the right axis represents the production temperature as a fraction of its initial value. The temporary increase in thermal drawdown above 1.0 reflects the initial period of thermal stabilization; as the surrounding rock formation warms, heat loss from the wellbore decreases, causing the production temperature to rise.**

This controlled outcome was achieved by adjusting key reservoir parameters relative to the GEOPHIRES Cape Station case study, as detailed in the following table:

| Parameter | GEOPHIRES Cape Station case study | Comment | This Analysis (FOAK & NOAK) | Comment |
|---|---|---|---|---|
| Fracture Height | 165.3 m | Based on total fracture surface area of 30 million ft² per well (Fercho et al., 2025) | 224 m | Fracture height of 224 m corresponds to ~43 million ft² per well, an ~43% increase from the reference value of 30 million ft² per well (Fercho et al., 2025). This is an optimistic but still overall plausible fracture size. Increased fracture sizes are also more likely to be achievable in granitic formations at greater depths (Ma et al., 2023). |
| Maximum Drawdown | 1.53% | Drawdown value that prevents minimum net electricity generation from going below 500 MWe | 5.31% | Allows more drawdown than Cape Station case study because the analysis is targeting a maximum total electricity generation dictated by plant design and a constant number of times redrilling (1–2). |

These parameters result in a single redrilling event across all FOAK scenarios and two events across all NOAK scenarios[4]. A difference in the assumed production flow rate between the two cost models — 60 kg/s per well for FOAK and 80 kg/s per well for NOAK — leads to a logical difference in number of required redrillings. The higher flow rate in the NOAK model accelerates heat extraction, necessitating two redrilling events over the project's lifetime, while the FOAK model requires only one.

**Capital Cost Models**

Drilling and Completion Cost Models

Two drilling and completion cost models were defined representing a higher-cost FOAK (First-of-a-Kind) estimate and a lower-cost NOAK (Nth-of-a-Kind) estimate.

The drilling and completion cost models were used to calculate the cost of vertical well sections and laterals (non-vertical sections). Vertical well section lengths correspond to the well depths associated with each BHT-gradient combination. Wells were modeled with a single 1440 meter lateral, based on Fervo's Project Red (Norbeck et al., 2024).

[4] See the "Number of times redrilling" metric in each cost model's detailed results.

Note that drilling and completion costs are included in the capital expenses for the initial wellfield. They are also used to calculate the drilling and completion portion of redrilling event costs, as described in Managing Thermal Drawdown and Redrilling Costs.

*FOAK: Top-Down Itemized*

FOAK costs were based on calculation of drilling rig rates using a top-down drilling strategy, with depth- and temperature-dependent ROP scaling calibrated to match available real-world drilling data.

For example, to drill to an 8 km depth, a standard rig would be used to drill the first 6 km. Then a heavy rig is used to drill the final 2 km.

***Rigs***

| Rig Type | Depth | Daily Rate | Base Rate | Spread | Power | Base ROP |
|---|---|---|---|---|---|---|
| Standard Rig | 0-6 km | $100k | $25k | $50-75k | 1500 HP | 45 ft/hr |
| Heavy Rig | 6-9 km | $175k | $75-100k | $50-75k | 2000 HP | 45 ft/hr |
| Super Heavy Rig | 9+ km | $350k | $200-250k | $100k | >3000 HP | 45 ft/hr |

***Temperature***

| Temperature | Incremental cost vs. baseline |
|---|---|
| <200°C | 0% |
| 200–300°C | +25% |
| >300°C | +100% |

***ROP Adjustment***

ROP (rate of penetration) was adjusted on a depth-dependent basis to calibrate the FOAK drilling and completion cost model to known real-world project drilling costs, designated as Calibration Points A and B, as follows:

| Calibration Point | Depth (km) | Bottom-Hole Temperature (°C) | Cost per Meter (USD) |
|---|---|---|---|
| A | 4.2672 | 220 | $1148 |
| B | 7.8 | 301 | $3346.15 |

| Depth | ROP Adjustment |
|---|---|
| $\leq 6$ km | $\dfrac{\text{Base ROP [ft/hr]}}{0.11 \cdot \text{Depth [km]} + 0.78}$ |
| $> 6$ km | $\dfrac{\text{Base ROP [ft/hr]}}{0.29 \cdot \text{Depth [km]} + 0.78}$ |

***Lateral costs***

A simplified per-meter cost model was used to compute the cost of the lateral sections as follows:

| Depth | Lateral cost |
|---|---|
| ≤ 5.5 km | $850/m |
| ≤ 9 km | $2381/m |
| > 9 km | $8840/m |

***Calculated Costs***

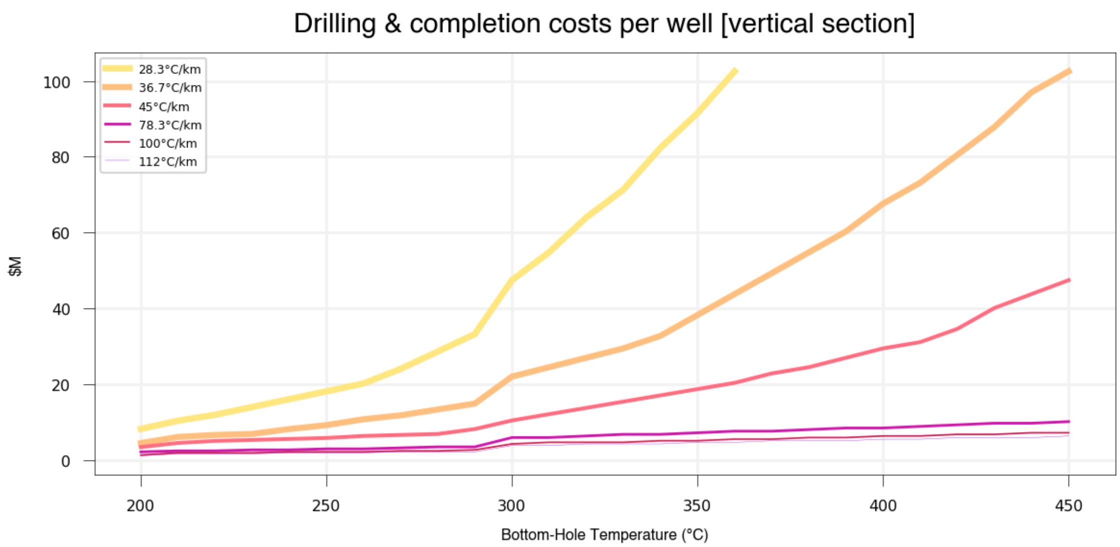


**Figure 8: FOAK drilling and completion costs per well vertical section**

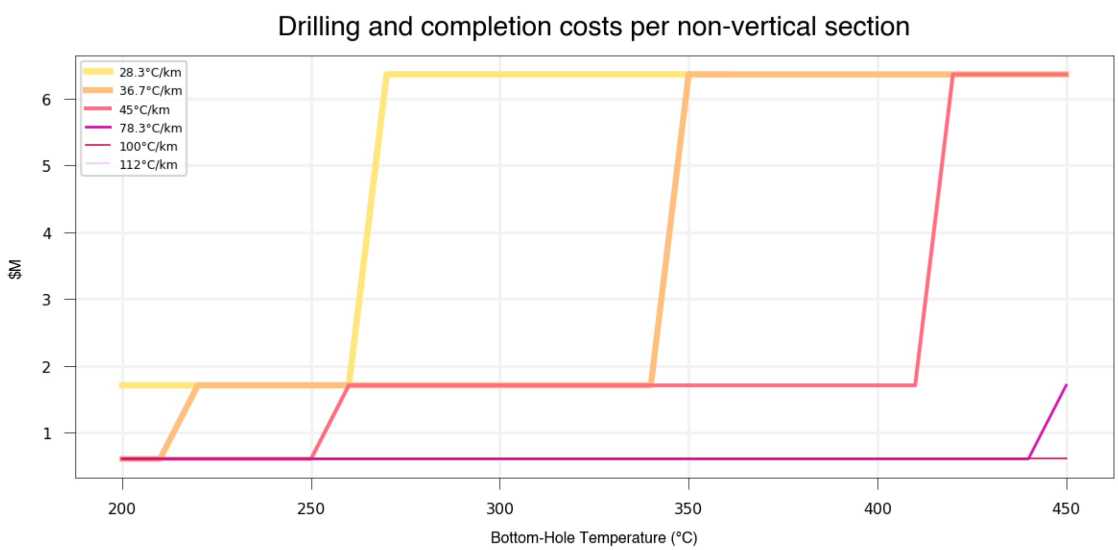


**Figure 9: FOAK drilling and completion costs per lateral (non-vertical section)**

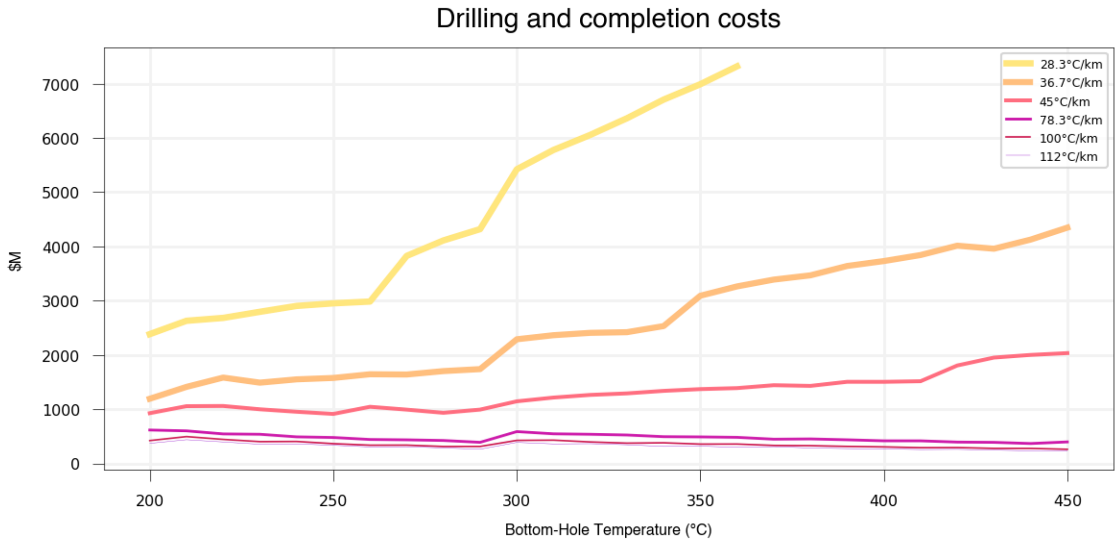


**Figure 10: FOAK total drilling and completion costs of all wells including both vertical and non-vertical (lateral) sections**

See Drilling Depth section for depths associated with each BHT-gradient combination.

*NOAK: Adjusted GeoVision Vertical Large Ideal Correlation*

The NOAK drilling and completion cost model was based on the GeoVision Vertical Large Ideal correlation (VERTICAL_LARGE_IDEAL) currently used in SAM/GETEM and GEOPHIRES[5] (DOE, 2019). Without adjustment, this correlation only accounts for depth (not temperature) and is not nominally intended to be applicable beyond 7km depth, but it may be representative of future cost reductions as high-temperature/high-depth drilling technologies are developed and commercialized.

To account for higher drilling costs associated with greater bottom-hole temperatures, an adjustment factor was applied to the VERTICAL_LARGE_IDEAL correlation value. The adjustment factor is defined by a monotonic cubic spline function based on the FOAK temperature incremental costs vs. baseline, which were additionally calibrated to ensure NOAK costs were less than FOAK, referred to as Reference Calibration Points in the following graph:

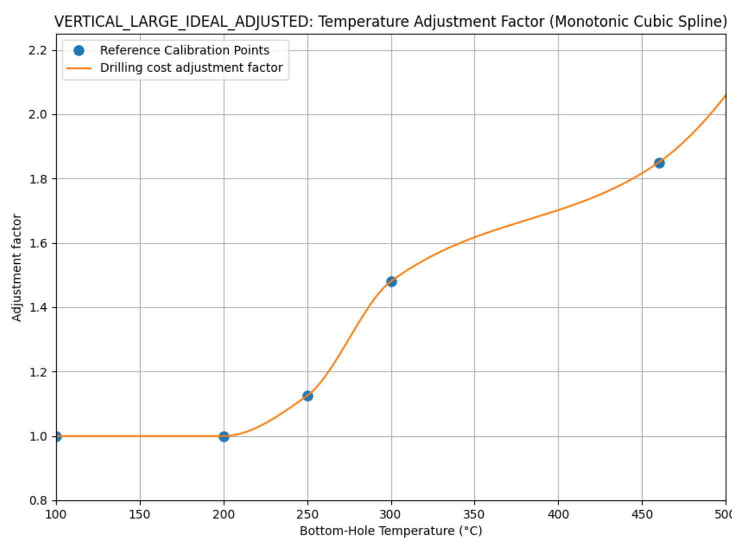


**Figure 11: Temperature adjustment factor for the NOAK drilling and completion cost model**

[5] Note that this correlation was re-evaluated and remained unchanged in NREL's 2025 drilling cost curve update.

For example, a scenario with a 3.7 km well depth and 78.3°C/km gradient has a bottom-hole temperature of 300°C. The VERTICAL_LARGE_IDEAL correlation produces a value of $3.26M per well vertical section in this scenario. With the application of an adjustment factor of 1.48 for the bottom-hole temperature = 300°C, the NOAK drilling and completion cost for the vertical section is $4.83M.

***Lateral costs***

Lateral costs were calculated with the GeoVision Deviated Large Ideal correlation (DEVIATED_LARGE_IDEAL), with the same adjustment factor applied.

***Calculated Costs***

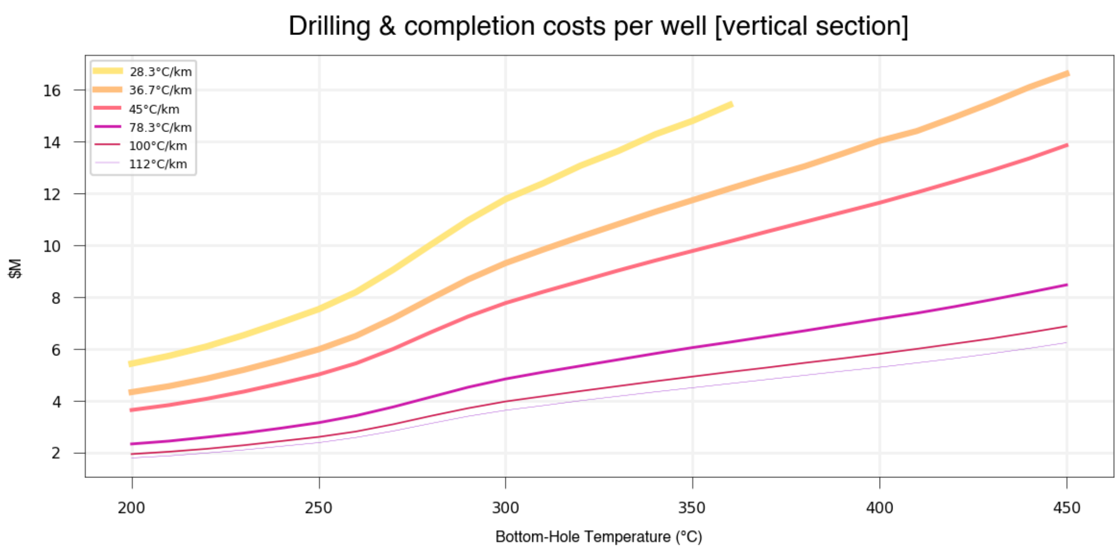


**Figure 12: NOAK drilling and completion costs per well vertical section**

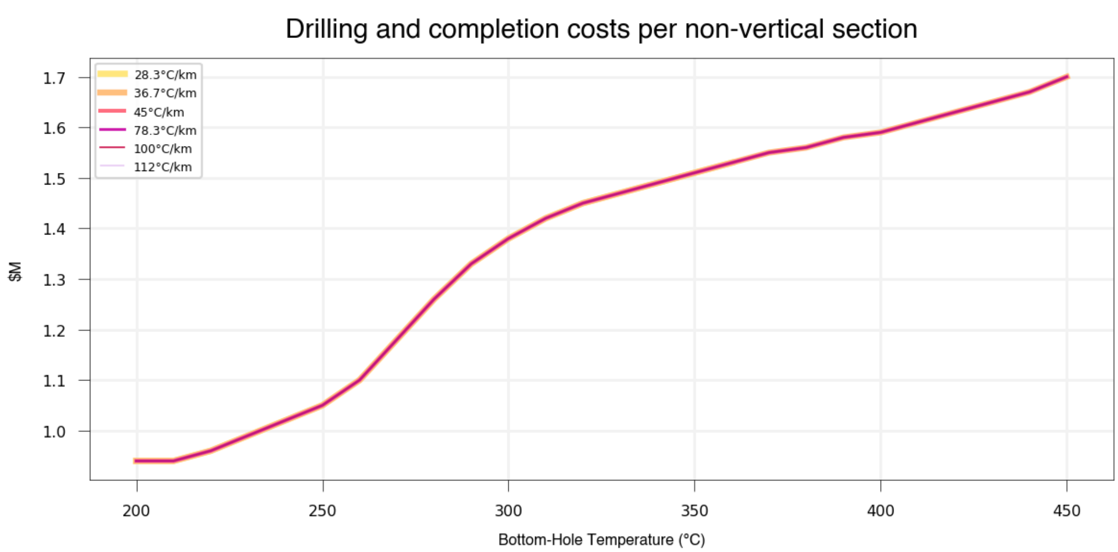


**Figure 13: NOAK drilling and completion costs per lateral (non-vertical section). Note that cost is constant for a given bottom-hole temperature across all gradients because the adjustment factor is temperature-dependent, and not depth-dependent.**

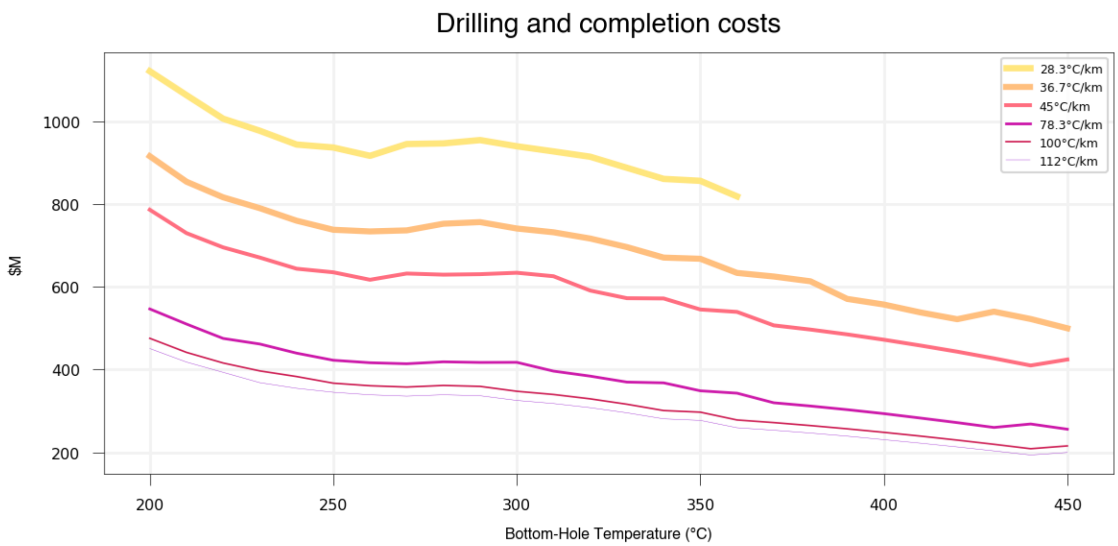


**Figure 14: NOAK total drilling and completion costs of all wells including both vertical and non-vertical (lateral) sections**

Stimulation Costs

Stimulation costs for FOAK and NOAK were modeled with an initial all-in cost of $4.6M per well ($4M baseline plus 15% contingency), matching the GEOPHIRES Cape Station case study (NREL, 2025). The initial cost then had an adjustment factor applied for bottom-hole temperature, similar to the adjustment factor applied in the NOAK drilling and completion cost model.

The initial all-in cost is based on a $4M baseline stimulation cost, calibrated from per-stage costs of high-intensity U.S. shale wells (Baytex Energy, 2024; Quantum Proppant Technologies, 2020), which are the closest technological analog for multi-stage EGS (Gradl, 2018). This baseline assumes standard sand proppant. The 15% contingency (~$0.6M) accounts for the necessary upgrade to ceramic proppant, which is required to resist mechanical crushing and geochemical degradation (diagenesis) over a 30-year well life at 200°C and above (Ko et al., 2023; Shiozawa & McClure, 2014).

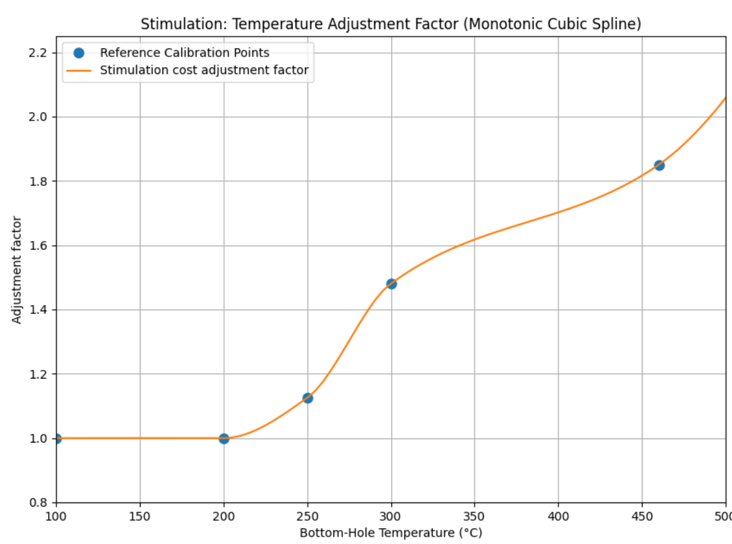


**Figure 15: Temperature adjustment factor for stimulation costs**

Surface Power Plant Design & Costs

A double-flash, 2x250 MW turbine plant design was used in both FOAK and NOAK scenarios for all BHTs. This design dictates the 500 MWe total electricity generation upper limit as described in the 500 MWe Power Plant Production Targeting methodology section. Note that for lower BHTs, a binary cycle plant would typically be used instead. This analysis modeled a double-flash plant design for all

BHTs to establish a consistent basis for comparison across temperature tranches; future work could explore the use of binary cycle plants for lower BHTs.

The plant costs in this analysis are derived from GEOPHIRES's built-in cost correlation for double-flash plants, which accounts for flow rate and temperature (NREL, 2025). An additional surface plant capital cost adjustment factor of 1.13 was then applied in order to calibrate the GEOPHIRES correlation with CATF's power production case study (Brown et al., 2024).

The power plant cost correlation was further modified for bottom-hole temperatures (BHTs) exceeding 359°C. The underlying GEOPHIRES correlation (Beckers & McCabe, 2019) is a polynomial function that accurately models declining per-kW costs for BHTs from 200–359°C. However, the function inflects beyond 359°C, predicting a cost increase. This inflection is an artifact of extrapolating the polynomial beyond its intended range. Based on personal consultation with the correlation's author, Koenraad Beckers, this artifact was corrected by fixing the surface plant capital cost at its minimum value of $664.94M for all BHTs greater than 359°C.

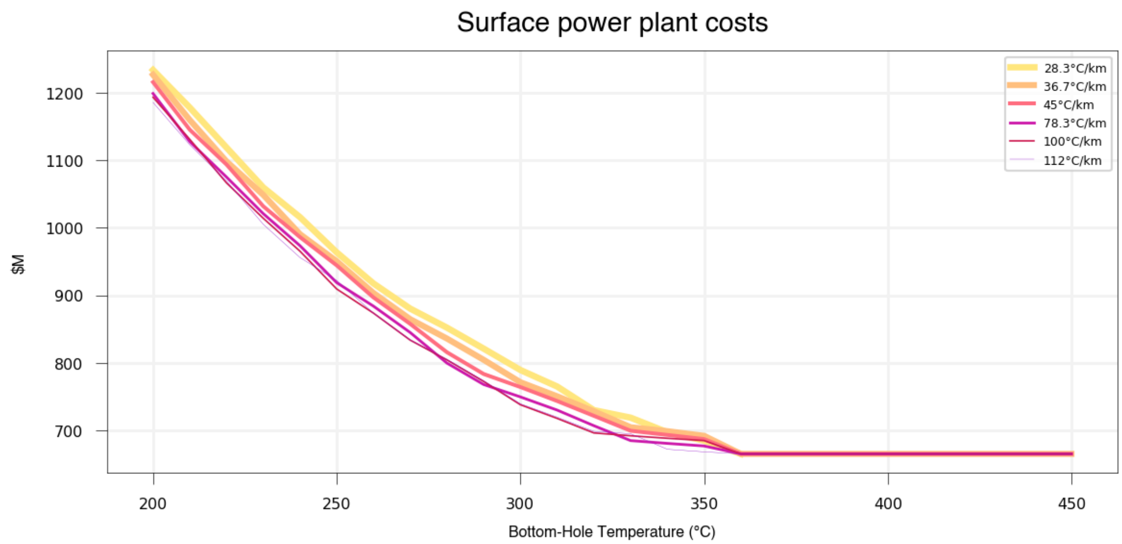


**Figure 16: Surface power plant costs by bottom-hole temperature, with capital cost adjustment factor and fixed cost for BHT >359°C**

**LCOE and Economic Metrics**

The primary economic metrics used in this analysis are the Levelized Cost of Electricity (LCOE) and the Internal Rate of Return (IRR). LCOE represents the average revenue per unit of electricity required to recover all costs over a plant's lifetime and is presented in U.S. cents per kilowatt-hour (¢/kWh). IRR is the discount rate at which the Net Present Value (NPV) of all project cash flows equals zero. In this analysis, LCOE is treated as the electricity breakeven price.

All financial metrics were calculated using the GEOPHIRES SAM Single Owner PPA Economic Model (NREL, 2025). These metrics include the primary indicators of LCOE and IRR, as well as additional metrics including Net Present Value (NPV), Multiple on Invested Capital (MOIC; sometimes referred to synonymously with ROI), and Profitability Index (PI; also referred to as the Value Investment Ratio (VIR) or profit investment ratio (PIR)). Some monetary values are reported in millions of U.S. dollars (MUSD).

The results presented are intended for a relative comparison of project economics across a range of temperatures and gradients under idealized conditions. Due to the reliance on modeled assumptions and extrapolated cost data, the absolute LCOE values should not be interpreted as predictive for any specific real-world EGS project. However, to provide a general benchmark for the modeled costs and point of comparison against hypothetical state-subsidized fossil fuel rates, figures and discussion include reference LCOE values of 4.4–6.5¢/kWh for coal and natural gas combined cycle (NGCC), based on NREL's 2022 Annual Technology Baseline (NREL, 2022).

## 3. RESULTS

**FOAK Results: Top-Down Itemized Drilling and Completion Cost Model**

Under the near-term, First-of-a-Kind (FOAK) cost model, the analysis indicates that achieving economic viability for unsubsidized EGS projects is a challenge across the entire temperature spectrum. The statistical overview shows that, on a gradient-weighted average basis, targeting hotter resources does not guarantee improved economics; in fact, the average LCOE for Hot and Superhot resources is 38% and 10% higher, respectively, than the baseline. This is primarily because the substantial increase in capital expenditure (CAPEX) required for deeper drilling often negates the thermodynamic benefits of higher temperatures, particularly in regions with lower geothermal gradients.

However, the detailed results reveal a crucial nuance: for rarer, high-quality gradients (≥78.3°C/km), economic viability is readily achievable, and profitability is maximized by targeting SHR temperatures. As shown in the NPV results, these high-gradient projects cross into positive NPV territory above approximately 220°C, with project value continuing to increase through the superhot range. This trend is the inverse of that seen for more common, lower gradients (≤45°C/km), where the high CAPEX required for deep drilling leads to a consistently negative NPV in regions without market subsidies such as tax credits, regulated market rates, and minimum clean and firm power requirements. This finding indicates that while broad EGS development is challenging under FOAK costs, near-term efforts can be profitable by strategically targeting high-gradient SHR resources.

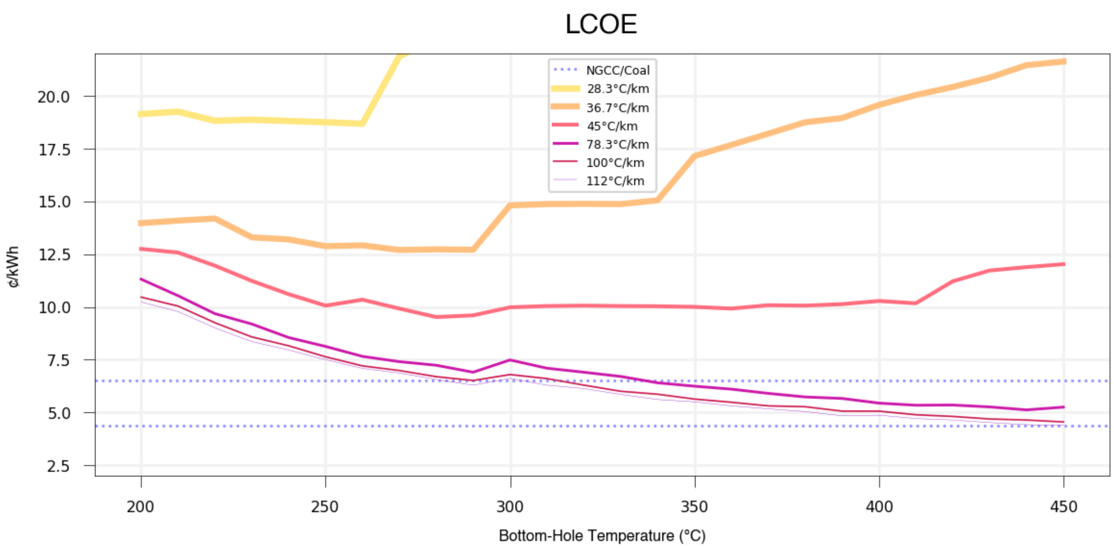


**Figure 17: FOAK LCOE (Electricity breakeven price) by BHT and gradient**

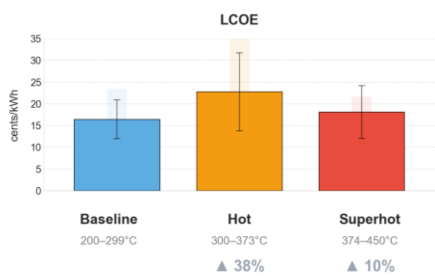


| | Mean | Std Dev | Min | Max |
|---|---|---|---|---|
| **Baseline** | 16.44 | 4.47 | 6.30 | 23.40 |
| **Hot** | 22.76 (+38%) | 8.99 | 5.18 | 35.10 |
| **Superhot** | 18.11 (+10%) | 6.06 | 4.40 | 21.60 |

**Figure 18: FOAK Statistical Overview for LCOE (Electricity breakeven price) (Gradient-Weighted; ¢/kWh)**

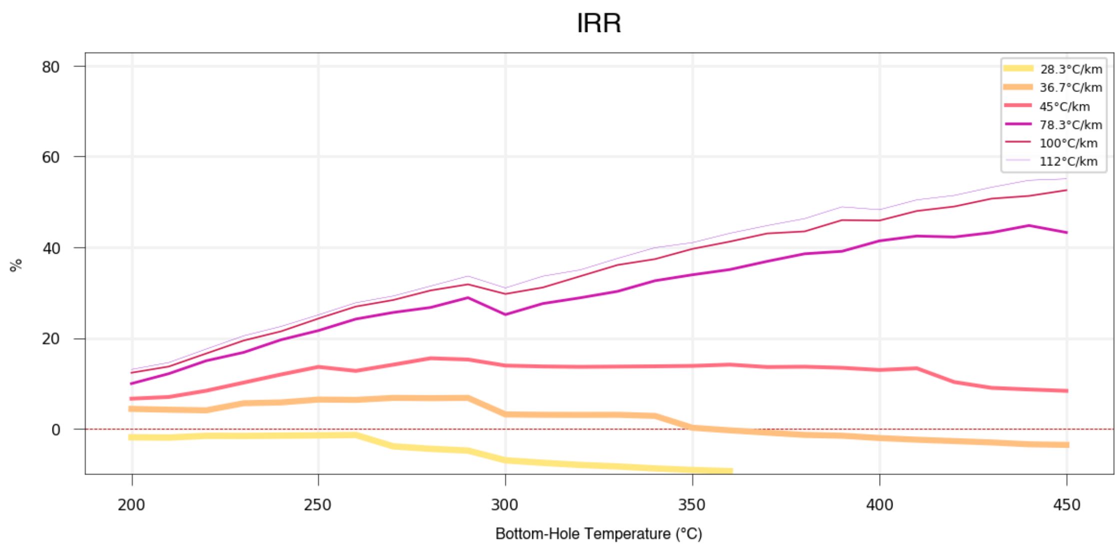


**Figure 19: FOAK IRR by BHT and gradient**

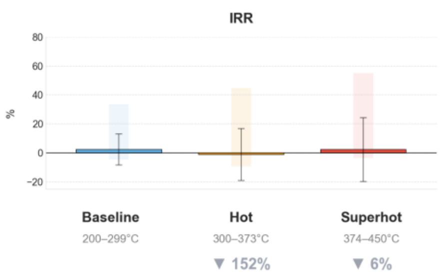


| | Mean | Std Dev | Min | Max |
|---|---|---|---|---|
| **Baseline** | 2.36 | 10.75 | -4.80 | 33.65 |
| **Hot** | -1.23 (-152%) | 17.97 | -9.33 | 44.77 |
| **Superhot** | 2.22 (-6%) | 21.98 | -3.54 | 55.06 |

**Figure 20: FOAK Statistical Overview for IRR (Gradient-Weighted; percent)**

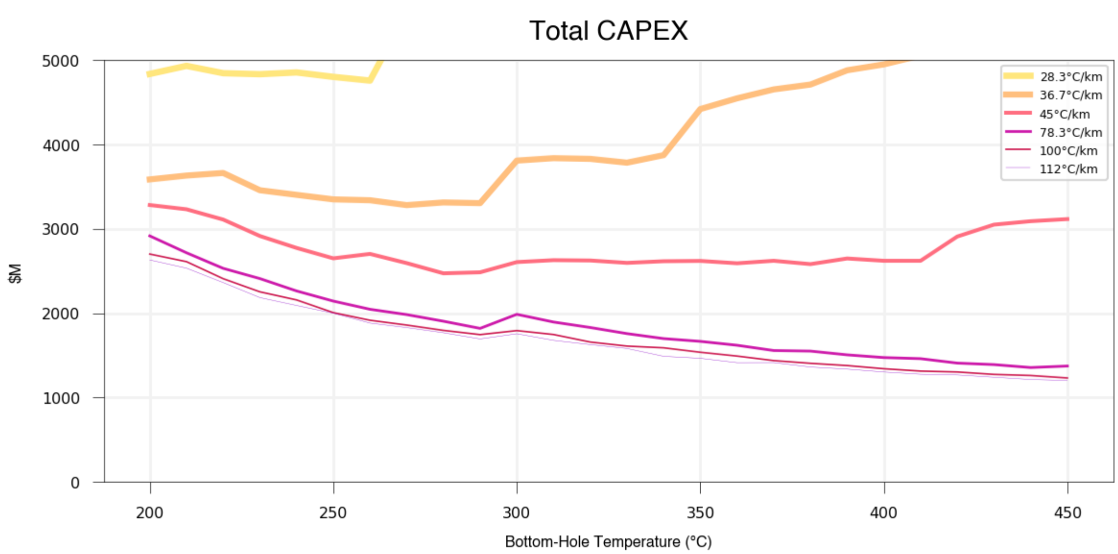


**Figure 21: FOAK Total CAPEX by BHT and gradient**

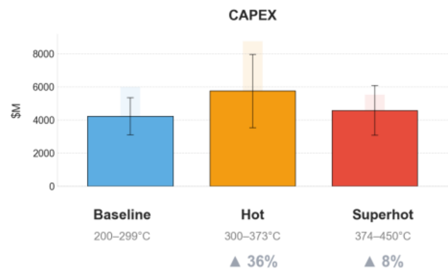


| | Mean | Std Dev | Min | Max |
|---|---|---|---|---|
| **Baseline** | 4225.49 | 1120.85 | 1694.32 | 5999.03 |
| **Hot** | 5753.97 (+36%) | 2218.83 | 1413.41 | 8752.78 |
| **Superhot** | 4584.23 (+8%) | 1497.49 | 1202.97 | 5539.24 |

**Figure 22: FOAK Statistical Overview for Total CAPEX (Gradient-Weighted; MUSD)**

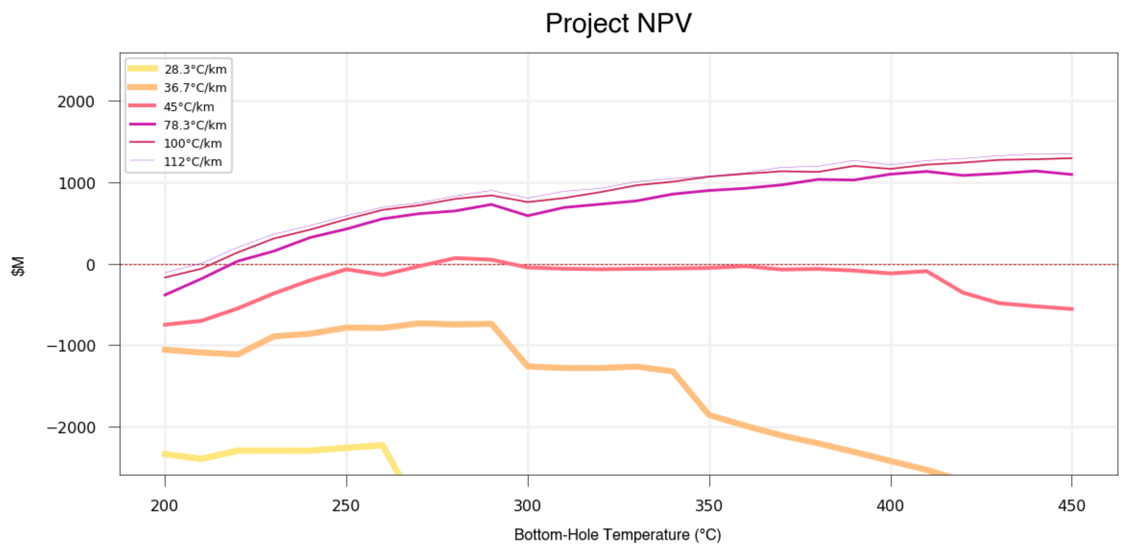


**Figure 23: FOAK Project NPV by BHT and gradient**

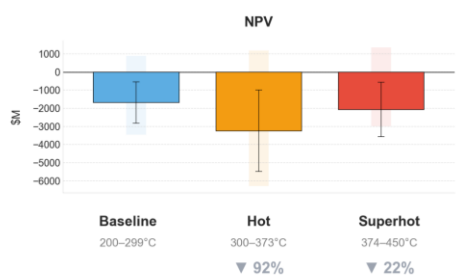


| | Mean | Std Dev | Min | Max |
|---|---|---|---|---|
| **Baseline** | -1688.28 | 1135.82 | -3457.20 | 898.64 |
| **Hot** | -3236.86 (+92%) | 2244.36 | -6274.80 | 1182.80 |
| **Superhot** | -2064.21 (+22%) | 1507.12 | -2976.80 | 1348.80 |

**Figure 24: FOAK Statistical Overview for Project NPV (Gradient-Weighted; MUSD)**

**NOAK Results: VERTICAL_LARGE_IDEAL_ADJUSTED Drilling and Completion Cost Model**

In the mature, Nth-of-a-Kind (NOAK) scenario, the economic outlook for EGS is transformed, with positive NPVs readily achievable across the gradient spectrum and SHR emerging as the clear economic leader. The gradient-weighted statistical overview shows a decisive advantage to targeting higher temperatures: SHR projects yield an LCOE that is 43% lower and an IRR that is 246% higher than the low-temperature baseline. This improvement is driven by a significant reduction in total capital expenditure (CAPEX) for hotter resources, as the higher power output per well drastically reduces the required well count and increases the relative efficiency of the surface equipment. (See Subsurface Results for further details.)

The detailed results underscore this potential for cost-competitiveness and profitability. The LCOE for SHR projects in high-gradient regions falls to between 3.84 and 4.85¢/kWh, values that are competitive with or lower than the reference LCOE for coal (4.4¢/kWh) and natural gas combined cycle plants (6.5¢/kWh) (NREL, 2022). This strong economic performance is directly linked to the enhanced efficiency of SHR systems; at 450°C, each production well contributes 36.0 MWe net, requiring fewer than 13 well pairs to achieve the 500 MWe plant target, in comparison to 81 well pairs contributing 5.8 MWe net for an equivalent 500 MW plant accessing a bottom-hole temperature of 200°C. Consequently, the IRR for high-gradient SHR projects becomes robust, indicating a highly favorable environment for investment in a mature EGS industry.

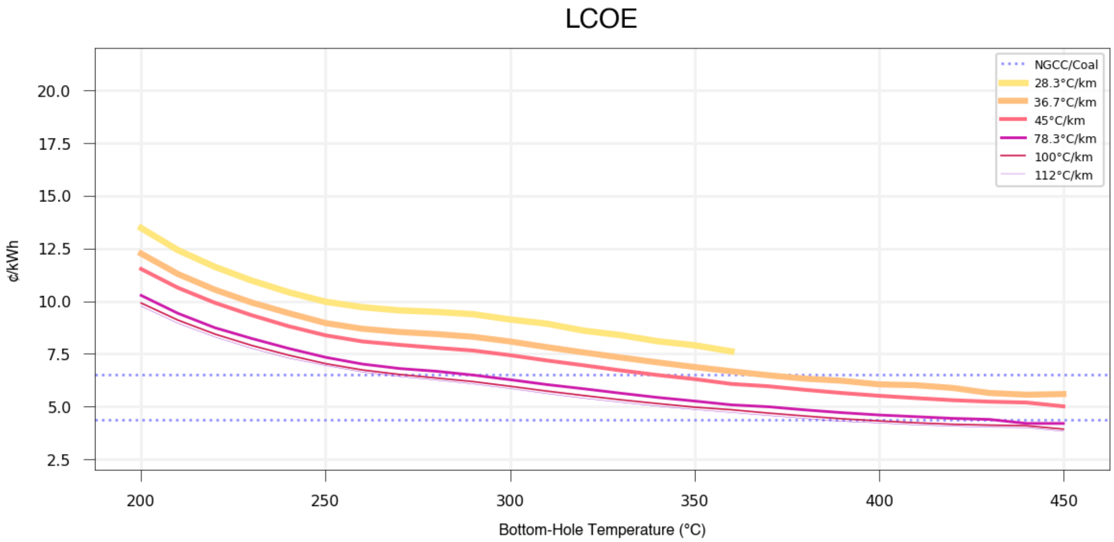


**Figure 25: NOAK LCOE (Electricity breakeven price) by BHT and gradient**

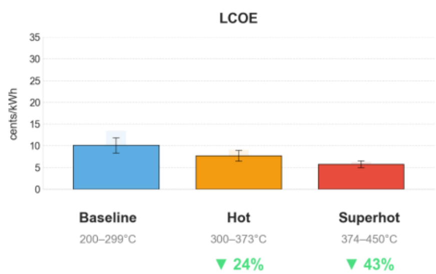


| | Mean | Std Dev | Min | Max |
|---|---|---|---|---|
| **Baseline** | 10.09 | 1.73 | 6.08 | 13.46 |
| **Hot** | 7.69 (-24%) | 1.25 | 4.58 | 9.13 |
| **Superhot** | 5.76 (-43%) | 0.74 | 3.84 | 6.33 |

**Figure 26: NOAK Statistical Overview for LCOE (Electricity breakeven price) (Gradient-Weighted; ¢/kWh)**

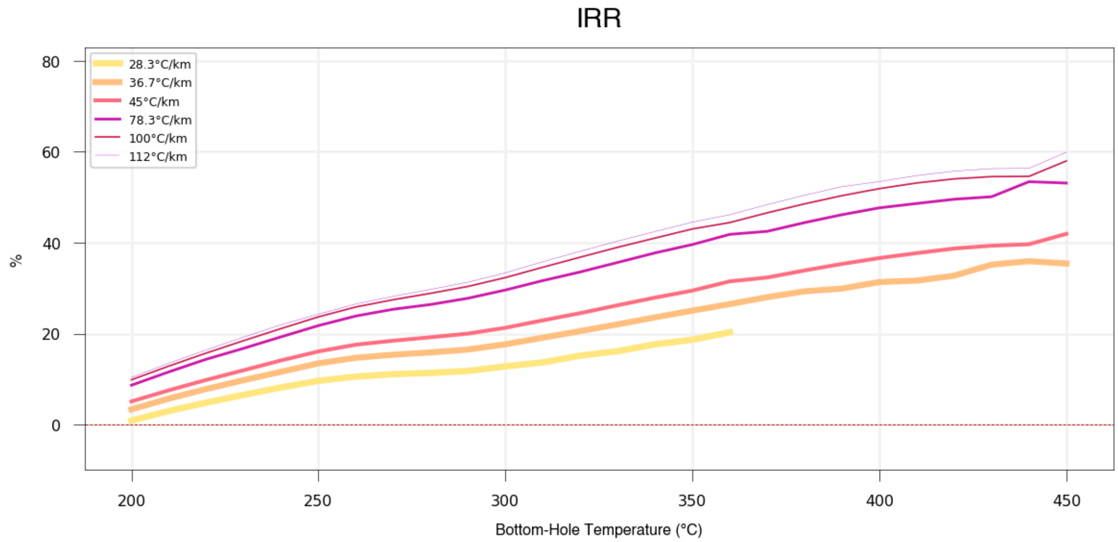


**Figure 27: NOAK IRR by BHT and gradient**

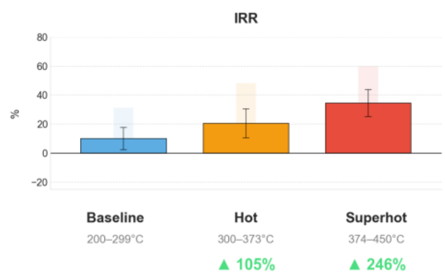


| | Mean | Std Dev | Min | Max |
|---|---|---|---|---|
| **Baseline** | 9.98 | 7.79 | 0.88 | 31.32 |
| **Hot** | 20.47 (+105%) | 10.00 | 12.79 | 48.37 |
| **Superhot** | 34.48 (+246%) | 9.24 | 29.30 | 59.90 |

**Figure 28: NOAK Statistical Overview for IRR (Gradient-Weighted; percent)**

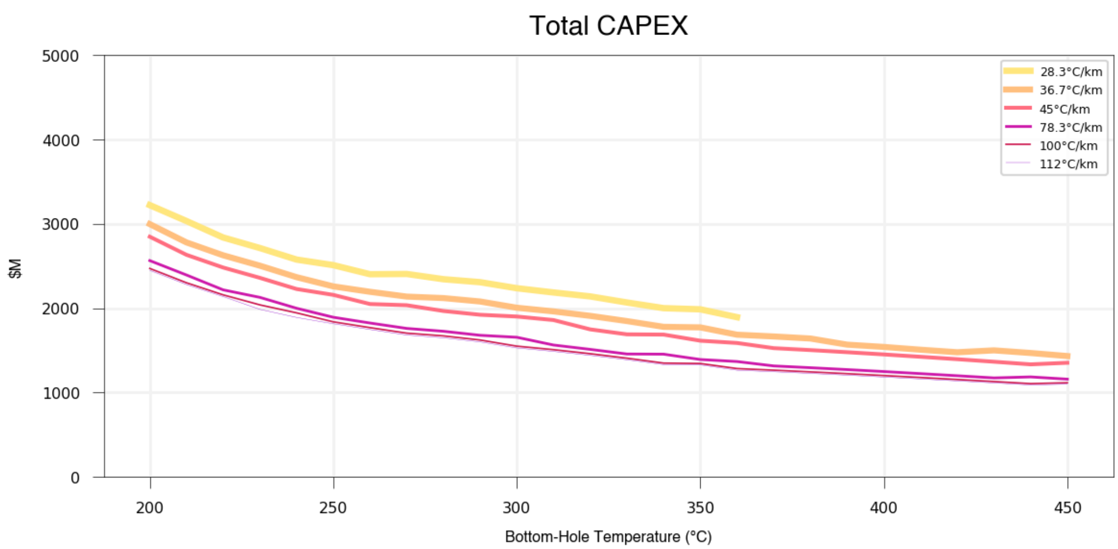


**Figure 29: NOAK Total CAPEX by BHT and gradient**

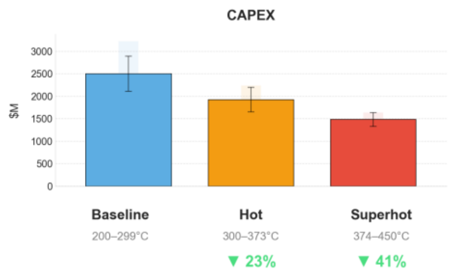


| | Mean | Std Dev | Min | Max |
|---|---|---|---|---|
| **Baseline** | 2500.98 | 388.73 | 1600.07 | 3218.43 |
| **Hot** | 1923.98 (-23%) | 273.28 | 1246.66 | 2235.26 |
| **Superhot** | 1483.80 (-41%) | 155.81 | 1090.28 | 1640.17 |

**Figure 30: NOAK Statistical Overview for Total CAPEX (Gradient-Weighted; MUSD)**

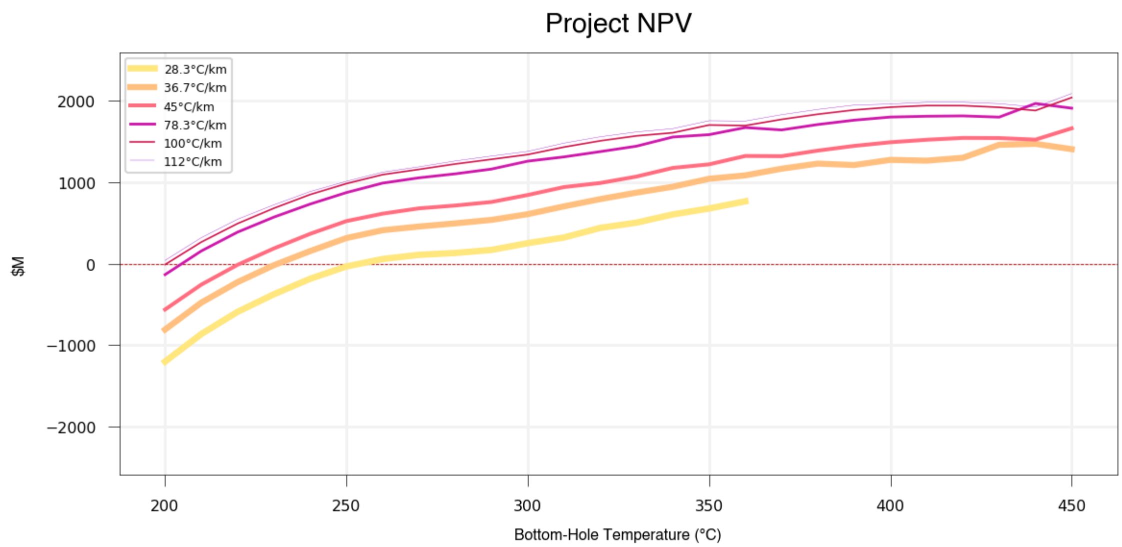


**Figure 31: NOAK Project NPV by BHT and gradient**

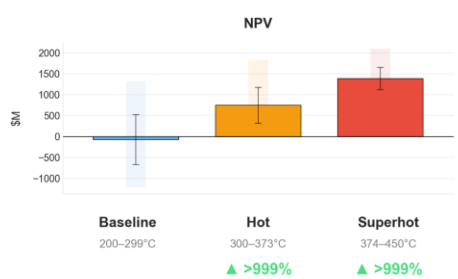


| | Mean | Std Dev | Min | Max |
|---|---|---|---|---|
| **Baseline** | -70.72 | 596.51 | -1205.00 | 1321.80 |
| **Hot** | 746.79 (-1156%) | 430.94 | 250.92 | 1830.30 |
| **Superhot** | 1385.10 (-2059%) | 262.40 | 1211.60 | 2090.70 |

**Figure 32: NOAK Statistical Overview for Project NPV (Gradient-Weighted; MUSD)**

**Subsurface Results**

<u>Number of Doublets & Per-Well Power Production</u>

As temperature increases, the required number of doublets (production/injection well pairs) decreases substantially across all gradients. This is because the increased enthalpy of the production fluid corresponds to a higher generation capacity per well, meaning fewer wells are needed to meet the 500 MWe target.

This effect is amplified in the NOAK scenario due to its higher assumed flow rate of 80 kg/s per well, compared to the FOAK scenario rate of 60 kg/s per well.

| BHT | Doublets (FOAK) | Net Power/Well (FOAK) | Doublets (NOAK) | Net Power/Well (NOAK) |
|---|---|---|---|---|

| BHT | Doublets (FOAK) | Net Power/Well (FOAK) | Doublets (NOAK) | Net Power/Well (NOAK) |
|---|---|---|---|---|
| 200°C | 110 | 4.4 MWe | 81 | 5.8 MWe |
| 450°C | 17 | 28.0 MWe | 13 | 36.0 MWe |

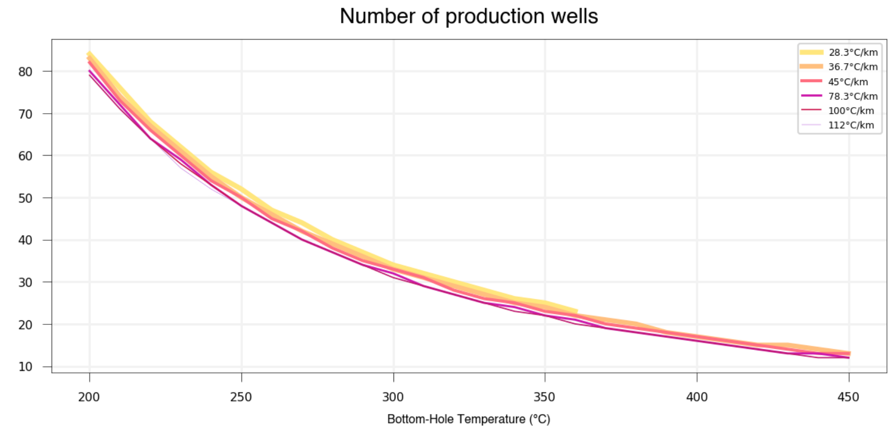


**Figure 33: NOAK number of production wells (equivalent to number of doublets)**

<u>Stimulation Costs</u>

Total stimulation costs also decrease substantially as temperature increases because of the reduced number of wells required. The initial all-in reservoir stimulation cost of $4.6M per well[6] was adjusted with a temperature-dependent factor as described in Methodology. Additional investigation to refine stimulation costs would be required to determine whether the trend found in this analysis remains when more detailed stimulation cost factors are considered, such as a depth-dependent factor.

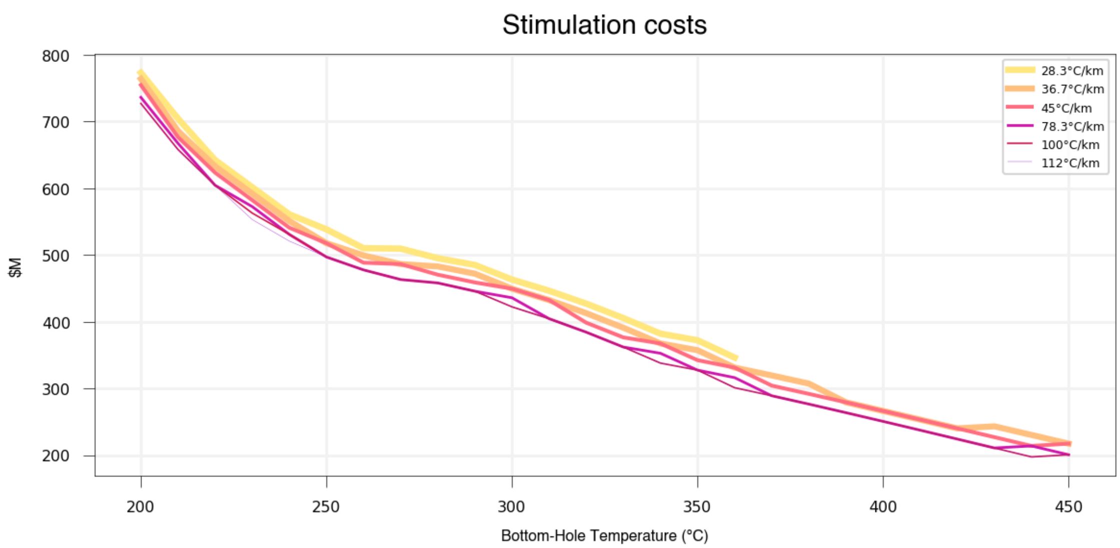


**Figure 34: NOAK stimulation costs**

**Pumping Power Results (Thermosiphoning)**

The analysis found a strong thermosiphoning effect as temperature increased, with required pumping power falling to 0 MW by 350°C for all gradients in both FOAK and NOAK scenarios. GEOPHIRES predicts this thermosiphoning because as BHT rises, the relative buoyancy of the superheated fluid in the well column eventually increases to the point where it overcomes gravity[7].

[6] See GEOPHIRES Case Study Documentation for Reservoir Stimulation Capital Cost per Well

[7] Note that for this study, GEOPHIRES's injectivity index pumping power model was used. The same effect is also predicted by the GEOPHIRES impedance pumping power model, which is applicable to binary cycle plants.

The occurrence of thermosiphoning in EGS systems is a debated topic among experts. Strong thermosiphoning has been observed in real-life closed-loop geothermal systems (CLGS) such as Eavor-Lite (Caceres, 2022). Thermosiphoning has been modeled for EGS systems (Wang et al., 2009), although some experts do not believe it would occur in a real-life EGS system. If thermosiphoning does not occur to the extent modeled in this analysis, parasitic load would not be decreased at higher temperatures and therefore reduce modeled economics herein for SHR EGS.

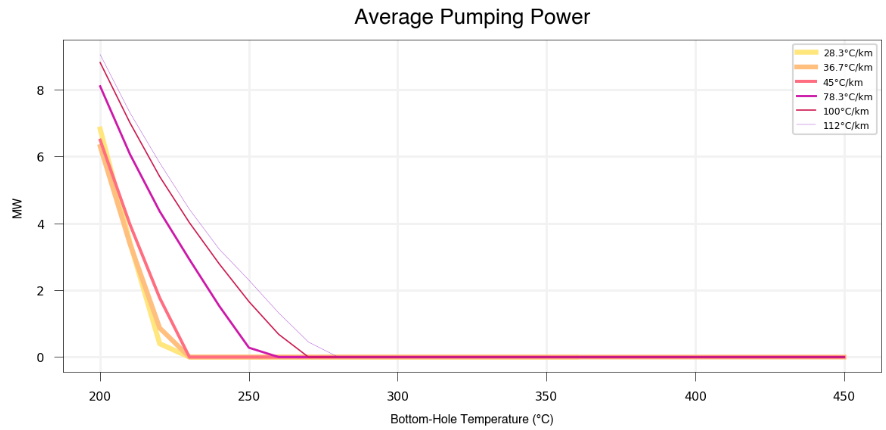


**Figure 35: Average pumping power for FOAK scenarios. NOAK scenarios follow the same relative trend but with slightly higher overall pumping power at the lower temperatures due to the increased flow rate.**

## 4. CONCLUSION

### Interpretation and Context of Findings

The primary finding of this analysis is that targeting superhot rock (SHR) resources yields substantially improved project economics for Enhanced Geothermal Systems (EGS) compared to lower-temperature resources. In mature, Nth-of-a-Kind (NOAK) scenarios, the model indicates that SHR EGS has the potential for an approximately 43% lower Levelized Cost of Electricity (LCOE) and a 246% higher Internal Rate of Return (IRR) compared to a 200°C baseline across all gradients[8]. This economic advantage is driven principally by the higher enthalpy of fluids produced from SHR reservoirs. As bottom-hole temperatures increase from 200°C to 450°C, the net power output per production well rises dramatically from ~5.8 MWe to 36.0 MWe in the NOAK model. This increased power density requires significantly fewer wells to achieve the target 500 MWe plant capacity, leading to a major reduction in total capital expenditure (CAPEX).

Importantly, the analysis indicates that SHR is not only a long-term goal. For geothermal gradients of 78.3°C/km or greater, SHR projects may yield compelling returns even under current First-of-a-Kind (FOAK) cost models, suggesting a viable strategy for near-term EGS development. The unsubsidized LCOE values achieved in high-gradient NOAK scenarios (3.84–4.85¢/kWh) position SHR EGS as a potential source of globally cost-competitive, zero-carbon, firm power.

### Limitations of the Study

While these findings are promising, the study relies on a set of simplifying assumptions and modeled conditions that represent key limitations and areas for future investigation.

1. Geofluid Chemistry: This study assumes a relatively benign geofluid suitable for a standard double-flash power plant. Hydrothermal SHR systems, particularly in magmatic settings, can produce corrosive fluids dependent on chemical composition, resulting in higher material costs (Karlsdottir, 2022). It is possible SHR EGS systems could be subject to similar challenges, although isolation of EGS working fluid from natural hydrological features may reduce the risk.

2. Simplified Stimulation Cost Model: While this analysis incorporates a temperature-dependent cost factor for reservoir stimulation to account for materials like ceramic proppants, the model remains a simplified correlation. It does not capture the full operational complexity of stimulating reservoirs under SHR conditions, where costs could vary significantly. Actual SHR stimulation could be more costly than for lower-temperature wells, representing a potential downside risk to the economic projections.

3. Extrapolated Cost Models: The analysis relies on the GEOPHIRES power plant cost correlation and extrapolated drilling cost curves. While adjusted for select first-order factors, these models do not necessarily capture the full range of site-specific engineering and geological challenges that an individual project may face.

[8] Weighted by gradient prevalence; see Gradient-Weighted Statistics in Methodology.

**Recommendations for Future Work**

The limitations of this study highlight several key areas for future research. Subsequent techno-economic analyses should incorporate geofluid chemistry as a primary variable, modeling distinct scenarios for different power plant technologies to establish a more realistic range of potential LCOE outcomes. The development of more granular, process-based stimulation and drilling cost models for deeper, high-temperature environments is needed to reduce uncertainty in these key cost categories. Finally, further research should focus on the impact of supercritical fluid properties on reservoir performance to refine projections for SHR EGS productivity and operational expenditures.

## ACKNOWLEDGEMENTS

This work was funded in part by the Clean Air Task Force (CATF). The author wishes to thank Terra Rogers at CATF for her valuable guidance and collaboration throughout the project. The author also wishes to thank his collaborators at the National Renewable Energy Laboratory (NREL) for their valuable input and continued partnership on the GEOPHIRES software, including Abra Gold, Dayo Akindipe, Hannah Pauling, and Mohammad Aljubran; and Jeff Bourdier for his diligent code review and open-source contributions to GEOPHIRES. Finally, thanks are extended to the subject matter experts whose feedback informed this analysis: Tony Pink for his expert input on drilling costs, Koenraad Beckers for his feedback on reservoir modeling and capital costs, and Gordon Brasnett for his insightful discussion and review.

## REFERENCES

Akindipe, D. and Witter. E. (2025). "2025 Geothermal Drilling Cost Curves Update". https://pangea.stanford.edu/ERE/db/GeoConf/papers/SGW/2025/Akindipe.pdf?t=1740084555

Augustine, C., Fisher, S., Ho, J., Warren, I., and Witter, E. (2023). *Enhanced Geothermal Shot Analysis for the Geothermal Technologies Office.* National Renewable Energy Laboratory. https://docs.nrel.gov/docs/fy23osti/84822.pdf

Baytex Energy. (2024). Eagle Ford Presentation. https://www.baytexenergy.com/content/uploads/2024/04/24-04-Baytex-Eagle-Ford-Presentation.pdf

Beckers, K. J. H. F. (2016). Low-temperature geothermal energy: Systems modeling, reservoir simulation, and economic analysis [Doctoral dissertation, Cornell University]. eCommons. https://ecommons.cornell.edu/bitstream/handle/1813/44328/kb447.pdf

Beckers, K. F., & McCabe, K. (2019). GEOPHIRES v2.0: updated geothermal techno-economic simulation tool. Geothermal Energy Science, 7(1), 3. https://doi.org/10.1186/s40517-019-0119-6

Bell, I. H., Wronski, J., Quoilin, S., Lemort, V. (2014). *Pure and Pseudo-pure Fluid Thermophysical Property Evaluation and the Open-Source Thermophysical Property Library CoolProp*. Industrial & Engineering Chemistry Research. https://doi.org/10.1021/ie4033999

Brown, D., Roy, C., Urbank, J., Hill, J., & Rogers, T. (2024). *Bridging the Gaps: A Survey of Methods, Challenges, and Pathways Forward for Superhot Rock Power Production*. Clean Air Task Force. https://cdn.catf.us/wp-content/uploads/2024/05/20144617/shr-bridging-gaps-power-production.pdf

Caceres, J.L. (2022). *Eavor's 'closed-loop' technology: Could this approach reach the 'holy-grail' status for clean energy?* Eavor Technologies Inc. https://eavor.com/blog/jose-luis-caceres-msc-eavors-closed-loop%E2%80%8B-technology-could-this-approach-reach-the-holy-grail%E2%80%8B-status-for-clean-energy/

Clark, C.E., Harto, C.B., Sullivan, J.L., & Wang, M.Q. (2010). *Water Use in the Development and Operation of Geothermal Power Plants* (Report No. ANL/EVS/R-10/5). Argonne National Laboratory. https://web.archive.org/web/20250202101145/https://www.energy.gov/eere/geothermal/articles/water-use-development-and-operations-geothermal-power-plants-0

Fercho, S., Norbeck, J., Dadi, S., Matson, G., Borell, J., McConville, E., Webb, S., Bowie, C., Rhodes, G. (2025). Update on the Geology, Temperature, Fracturing, and Resource Potential at the Cape Geothermal Project Informed by Data Acquired from the Drilling of Additional Horizontal EGS Wells. *Proceedings, 50th Workshop on Geothermal Reservoir Engineering*. Stanford University, Stanford, California, SGP-TR-229. https://pangea.stanford.edu/ERE/pdf/IGAstandard/SGW/2025/Fercho.pdf

Gradl, C. (2018). Review of Recent Unconventional Completion Innovations and their Applicability to EGS Wells. Stanford Geothermal Workshop. https://pangea.stanford.edu/ERE/pdf/IGAstandard/SGW/2018/Gradl.pdf

Gringarten AC, Witherspoon PA, Ohnishi Y. Theory of heat extraction from fractured hot dry rock. J Geophys Res. 1975;80(8):1120–4.

Karlsdottir, S. N. (2022). Corrosion, Scaling and Material Selection in Geothermal Power Production. Faculty of Industrial Engineering, Mechanical Engineering and Computer Science , University of Iceland. https://doi.org/10.1016/B978-0-12-819727-1.00106-0

Ko, S., Ghassemi, A., & Uddenberg, M. (2023). Selection and Testing of Proppants for EGS. Proceedings, 48th Workshop on Geothermal Reservoir Engineering, Stanford University, Stanford, California. https://pangea.stanford.edu/ERE/db/GeoConf/papers/SGW/2023/Ko.pdf

Ma, X., Wang, Gl., Hu, Dw. et al. Hydraulic fracturing of granite under real-time high temperature and true triaxial stress. J. Cent. South Univ. 30, 243–256 (2023). https://doi.org/10.1007/s11771-023-5221-z

Naganawa, S., Tsuchiya, N., Okabe, T., Kajiwara, T., Shimada, K., & Yanagisawa, N. (2017). Innovative Drilling Technology for Supercritical Geothermal Resources Development. Proceedings of the 42nd Workshop on Geothermal Reservoir Engineering (SGP-TR-212), Stanford, CA. https://pangea.stanford.edu/ERE/pdf/IGAstandard/SGW/2017/Naganawa.pdf

National Renewable Energy Laboratory. (2022). 2022 Annual Technology Baseline. https://web.archive.org/web/20230115203605/https://atb.nrel.gov/electricity/2022/index

National Renewable Energy Laboratory. (2024). 2024 Annual Technology Baseline: Geothermal. https://atb.nrel.gov/electricity/2024/geothermal

National Renewable Energy Laboratory. (2025). GEOPHIRES (Version 3.9) [Computer software]. https://github.com/NREL/GEOPHIRES-X

National Renewable Energy Laboratory. (2025). GEOPHIRES Case Study: 500 MWe EGS Project Modeled on Fervo Cape Station. GEOPHIRES Documentation. Retrieved June 25, 2025, from https://nrel.github.io/GEOPHIRES-X/Fervo_ProjectCape-4.html

National Renewable Energy Laboratory. (2025). SAM Economic Models. In GEOPHIRES Documentation. Retrieved October 7, 2025, from https://nrel.github.io/GEOPHIRES-X/SAM-Economic-Models.html

National Renewable Energy Laboratory. (2017). Geothermal prospector. Retrieved 2024, from https://maps.nrel.gov/?da=geothermal-prospector

Norbeck, J., Gradl, C., Latimer, T. (2024, September 10). Deployment of Enhanced Geothermal System Technology Leads to Rapid Cost Reductions and Performance Improvements. https://doi.org/10.31223/X5VH8C

Quantum Proppant Technologies. (2020). Well Completion Technology. World Oil. https://quantumprot.com/uploads/images/2b8583e8ce8038681a19d5ad1314e204.pdf

Ramey HJ Jr. Wellbore heat transmission. J Petrol Technol. 1962;14(04):427–35.

Reinsch, T., Dobson, P., Asanuma, H. et al. (2017). Utilizing supercritical geothermal systems: a review of past ventures and ongoing research activities. Geotherm Energy 5, 16. https://doi.org/10.1186/s40517-017-0075-y

Scott, S., Driesner, T. & Weis, P. (2015). Geologic controls on supercritical geothermal resources above magmatic intrusions. Nat Commun 6, 7837. https://doi.org/10.1038/ncomms8837

Shiozawa, S., & McClure, M. (2014). EGS Designs with Horizontal Wells, Multiple Stages, and Proppant. ResFrac. https://www.resfrac.com/wp-content/uploads/2024/07/Shiozawa.pdf

United Nations Economic Commission for Europe. (2022). *Supplementary Specifications for the application of the United Nations Framework Classification for Resources (Update 2019) to Geothermal Energy Resources*. https://unece.org/sites/default/files/2022-12/UNFC_Geothermal_Specs_25October2022.pdf

United States, Department of Energy, Geothermal Technologies Office. GeoVision: Harnessing the Heat Beneath Our Feet. U.S. Department of Energy, 2019, https://www.energy.gov/sites/prod/files/2019/06/f63/GeoVision-full-report-opt.pdf.

Wang, Z., McClure, M. W., & Horne, R. N. (2009). A Single-Well EGS Configuration Using a Thermosiphon. In Proceedings, Thirty-Fourth Workshop on Geothermal Reservoir Engineering. Stanford, CA: Stanford University. Retrieved from https://earthsciences.stanford.edu/ERE/pdf/IGAstandard/SGW/2009/wang.pdf